Progress in Medical Devices
ISSN: 2957-5478

Zentime

Research Article https://doi.org/10.61189/804304ntkyxb

Investigation of water-assisted colonoscopy using a constant-temperature water infusion system

Hongsheng Li[1*], Chunhua Zhou[2*], Taojing Ran[2*], Yao Zhang[2], Xiaonan Shen[2], Shiju Yan[1], Duowu Zou[2]

[1]School of Health Science and Engineering, University of Shanghai for Science and Technology, Shanghai 200093, China. [2]Department of Gastroenterology, Ruijin Hospital, Shanghai Jiao Tong University School of Medicine, Shanghai 200025, China.
[*]The authors contribute equally.

Corresponding authors: Duowu Zou and Shiju Yan.

Acknowledgments: This work was supported by the Medical Engineering Cross-disciplinary Project Special Fund of Ruijin Hospital, Shanghai Jiao Tong University School of Medicine, and the University of Shanghai for Science and Technology.

Declaration of conflict of interest: None.

Received February 15, 2025; Accepted June 18, 2025; Published September 30, 2025

Highlights

- Developed a 37 °C constant-temperature electronic control module, including circuit board design and selection of electronic components, ensuring stable and reliable temperature control for the water infusion system.
- Evaluated and optimized the layout and selection of pipelines and valves, ensuring secure, leak-proof water connections, precise valve flow directions, and rapid, reliable valve operation.
- Designed an efficient tailored to the dimensions and shape of the water reservoir, determining optimal parameters including heating power, structural configuration, size, and placement.

Abstract

Background: Colonoscopy is a key technique for the prevention and early detection of colorectal cancer. Water-assisted colonoscopy is increasingly adopted due to its potential to reduce patient discomfort. However, the temperature of the infused water plays a crucial role in both procedural quality and patient experience. This study aimed to optimize water-assisted colonoscopy by developing a constant-temperature water infusion system. **Methods:** A two-dimensional finite element model was established using COMSOL Multiphysics to simulate the heat transfer process between the heating base and the liquid container. The system consisted of a medical-grade 304 stainless steel container, a nichrome heating wire embedded in rubber, and an integrated piping network. Quadrilateral meshing was applied to short-range solid–liquid interfaces and triangular meshing elsewhere, resulting in detailed modeling for both natural heating (27,801 elements) and circulation heating (43,998 elements). Based on simulation results, a hardware platform was developed to deliver sterile water at a constant temperature of 37 °C for digestive endoscopic procedures. **Results:** Circulation heating demonstrated superior thermal efficiency and more uniform temperature distribution than natural heating. Under ambient conditions (25 °C), the system reliably maintained water temperature at (37±1)°C . Partitioned meshing enhanced computational precision with a minimum element size of 0.1 mm. Solid-liquid coupling analysis confirmed stable heat conduction during dynamic infusion. The device allows for independent temperature presetting and stepless flow rate adjustment via a control panel. It is also compatible with standard endoscopic systems, thereby enhancing procedural efficiency and safety. **Conclusion:** The proposed constant-temperature water infusion system model offers a reliable and adaptable solution for water-assisted colonoscopy, improving both diagnostic performance and patient comfort through precise thermal regulation.

Keywords: Water-assisted colonoscopy, constant-temperature control, finite element analysis, thermodynamic simulation, medical device design

Address correspondence to: Duowu Zou, Department of Gastroenterology, Ruijin Hospital, Shanghai Jiao Tong University School of Medicine, No. 227 South Chongqing Road, Huangpu District, Shanghai 200025, China. E-mail: zdw_pi@163.com. **Shiju Yan**, School of Health Science and Engineering, University of Shanghai for Science and Technology, No. 516 Jungong Road, Yangpu District, Shanghai 200093, China. Tel: +86-021-55271115. E-mail: yanshiju@usst.edu.cn.

Introduction

Colorectal cancer remains a significant global public health concern, especially in developing countries. Early detection and prevention through screening colonoscopy are essential strategies for reducing both the incidence and mortality associated with colorectal cancer [1, 2]. The detection and removal of precancerous polyps during colonoscopy have been proven to be effective in preventing the progression to colorectal cancer [3]. However, conventional colonoscopy techniques that utilize air insufflation often cause considerable patient discomfort, leading to decreased adherence to screening recommendations. Such discomfort may include abdominal pain, bloating, and overall intolerance to the procedure, potentially discouraging patients from undergoing necessary follow-up examinations [4, 5].

Although sedation and analgesia are commonly employed during colonoscopy, the use of propofol and other anesthetic agents is generally not recommended for patients with significant comorbidities or high-risk profiles. Additionally, some patients require the presence of a family member during anesthetized procedures, followed by a recovery period, which may pose logistical challenges. In recent years, water-assisted colonoscopy (WAC) has emerged as a promising alternative to conventional air insufflation techniques [6-8]. WAC methods are generally classified into two main types: water immersion and water exchange [9]. The efficacy of WAC has been validated in multiple randomized controlled trials [10, 11]. A recent meta-analysis reported that the water exchange method achieved the highest adenoma detection rate, particularly in the right colon and in colorectal cancer screening cases [12].

Additionally, the Boston Bowel Preparation Scale scores were significantly higher with water exchange. This technique was also associated with a higher proportion of unsedated examinations and reduced real-time insertion pain, making it the least painful insertion method and potentially improving procedural accessibility and cost-effectiveness. Investigations have examined the impact of water temperature on procedural outcomes. Instilling room-temperature water into the rectosigmoid colon has been linked to increased mucus secretion, necessitating additional cleansing during withdrawal [13]. A double-blind randomized trial comparing cool versus warm water immersion demonstrated that, while both approaches were effective, warm water provided advantages in reducing the need for auxiliary maneuvers [14]. These findings suggest that maintaining infused water at body temperature (37 °C) may enhance both patient comfort and procedural efficiency.

The challenge of maintaining constant water temperature during colonoscopy has generated increasing interest in the development of automated temperature control systems. These systems need to be precise, reliable, and capable of sustaining stable temperatures throughout the entire procedure [15, 16]. The integration of modern technologies-such as embedded controllers and high-precision temperature monitoring systems-offers promising solutions to address this challenge.

Numerical simulation

System modeling

The interaction between the heating chassis and the liquid container was investigated using finite element simulations conducted in COMSOL Multiphysics. The objective was to generate simulation data to support the design of a constant-temperature water infusion system. Considering the complexity of the solid-liquid coupling problem-particularly regarding real-time performance and computational efficiency-a two-dimensional model was employed to simplify the heating system. This approach effectively reduced model complexity and significantly shortened computation time, while preserving the reliability of simulation outcomes. Given the minimal wall thickness of the hose (only 1-1.2 mm), its impact on the overall thermodynamic behavior of the solid-liquid system was considered negligible. Therefore, hose wall was further simplified as a thin boundary layer. Additionally, the container shell was modeled as a heat transfer interface to simulate thermal conduction.

The finite element model used in this simulation, as illustrated in **Figure 1**, is divided into two sections. The left panel shows the key components of the thermostatic heating system, including the liquid container, heating plate, and piping network. The right panel presents the geometric dimensions of the model.

By removing the piping system, a natural heating model was developed to facilitate a comparative analysis of heat conduction and fluid dynamics between the two configurations. The liquid container is cylindrical, with a bottom diameter labeled as R, an overall height of H,

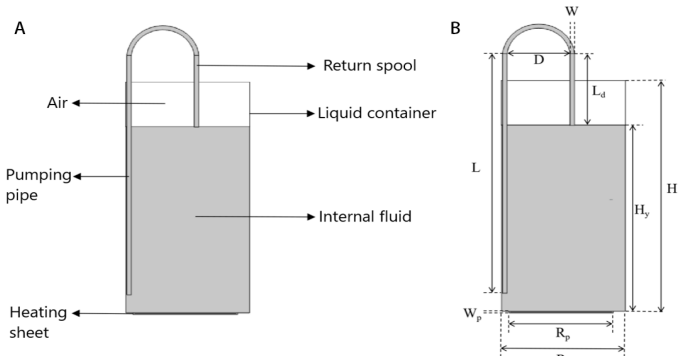

Figure 1. Finite element model used for thermal simulation. (A) Structural layout of the model; (B) Geometric dimensions of the model.

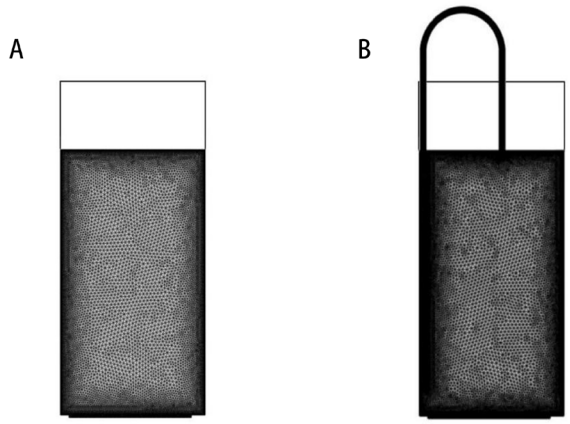

Figure 2. Mesh division of the water infusion container model. (A) Natural heating mode; (B) Circulating heating mode.

and a liquid height of H_y. The bottom heating plate is disc-shaped, with a diameter of R_p and a thickness of W_p. The integrated piping system comprises both long and short pipes, each with a diameter W, lengths L and L_d, respectively, and an inter-pipe spacing denoted as D. Detailed geometric parameters for each component were defined during model construction to ensure both accuracy and practical relevance. The specific values of these parameters are provided in **Table 1**.

To ensure precise temperature control and enhance heat transfer efficiency, the liquid container was fabricated using medical-grade 304 stainless steel. The housing of the heating element was made of rubber, with a nickel–chromium alloy heating wire embedded inside. Based on these materials and structural characteristics, simulations were conducted to analyze temperature distribution and heat flow dynamics during the heating process. Further details of these parameters are provided in **Table 2**.

The simulation analysis in this study incorporated multiple physical fields, including fluid flow and multiphysics coupling. The initial phase of the thermal boundary condition analysis involved defining the external air environment and the internal physiological saline, as well as setting the initial temperature of all system components to 25 °C. Calculations were performed using the finite element method, specifically employing the turbulence and solid-liquid coupling modules.

The finite element simulation in this study focused on heat conduction and fluid flow phenomena near the short-distance interface where solid–liquid contact occurs. A differentiated meshing strategy was employed, applying quadrilateral meshing to the contact edge regions and triangular meshing to the remainder of the model. Particular attention was given to the rubber heating sheet, silicone tubing, and normal saline, with finer mesh refinement applied to these critical components. The mesh distribution of the model is illustrated in **Figure 2**. For the natural heating mode, the model consisted of 27,801 domain elements and 1,016 boundary elements, with a minimum element size of 0.2 mm. In the circulating heating mode, the mesh comprised 43,998 domain elements and 2,133 boundary elements, with a minimum element size of 0.1 mm.

Simulation data analysis

This study examined temperature variations during natural and circulating heating processes to evaluate differences in heating efficiency and temperature distribution. Simulation results were analyzed to visualize the temperature fields at three critical time points (0.1 h, 0.14 h, 0.18 h) using thermal cloud maps, as shown in **Figures 3**, **4**, and **5**. In the natural heating mode, the heating sheet rapidly heated up and transferred heat to the bottom of the container, eventually reaching the lower layer of the liquid. However, this process resulted in an uneven temperature distribution within the liquid, with a notable temperature gradient between the bottom and upper middle layers, even when the bottom temperature approached the target value of 37 °C at 0.18 h.

In contrast, the circulating heating mode-

Table 1. Geometric parameters of the water infusion container model

Parameter	R	H	H_y	R_p	W_p	W	L	L_d	D
Value (mm)	140	280	220	120	2	6	300	100	70

Table 2. Thermophysical properties of four different materials used in the heating system

Property	304 Stainless Steel	Rubber	Nichrome	Normal Saline
Density (kg/m^3)	7,930	1,100	8,400	1,000
Melting Point (℃)	1,398	177	1,400	-0.5
Electrical Conductivity (S/m)	1.45×10^{-6}	1.0×10^{-10}	1.2×10^{-6}	1.553
Thermal Conductivity (W/m·K)	16.3	0.5	30	0.6
Specific Heat Capacity (J/kg·K)	500	1,300	440	4,200

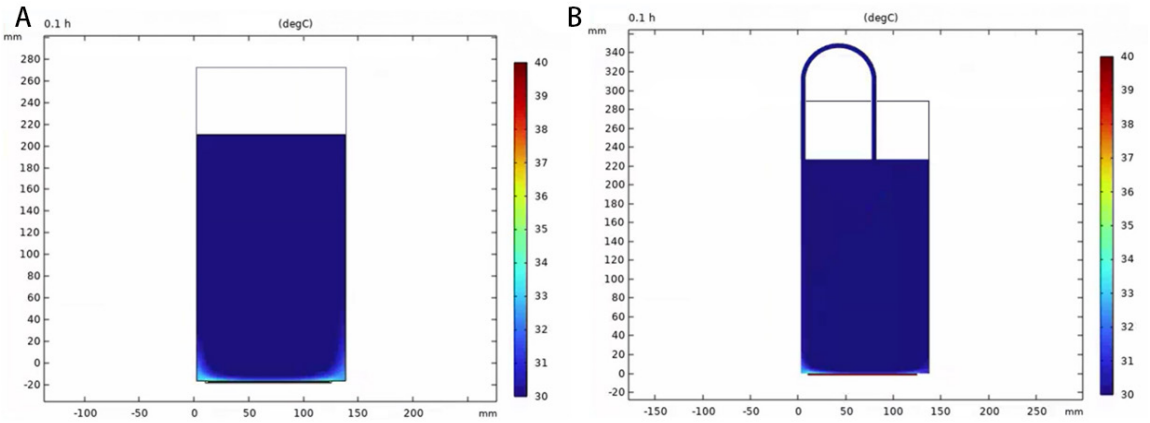

Figure 3. Heat distribution in the water infusion container model at 0.1 h. (A) Natural heating mode; (B) Circulating heating mode.

enabled by a closed-loop pipe and valve system-demonstrated more uniform heat distribution and improved temperature control. The circulating system reached the target temperature more rapidly than the natural heating mode, highlighting its superior thermal efficiency.

System development

The system developed in this study consists of three main components: the circuit control system, the external working devices, and the mechanical control system. A schematic representation of the constant temperature test platform is shown in **Figure 6**. The circuit control system includes several key components, such as a central processor for data processing, a heating system with a proportional-integral-derivative (PID) adaptive algorithm, a multi-channel real-time temperature measurement circuit, an efficient water level alarm system, a stable power supply module, and a multifunctional human-computer interaction panel. Additionally, it features various control instructions and communication modules to facilitate system operation. The external working devices include sensors and heating elements specifically designed for the liquid container. These components transmit signals to the circuit control system in real time, enabling dynamic adjustments to the heating process according to programmed instructions. The mechanical control system is responsible for regulating the valve channels and pump speeds, ensuring smooth switching between injection modes and enabling precise control of the liquid flow rate within the container and pipes.

Hardware design

Main control circuit

The STM32F103ZET6 was selected as the main control chip for this study. With improvements in key performance metrics such as data conversion rate, storage capacity, operating temperature range, power consumption, and interface functionality, this chip provides enhanced performance and flexibility, making it ideal for complex embedded applications [17].

Heater element

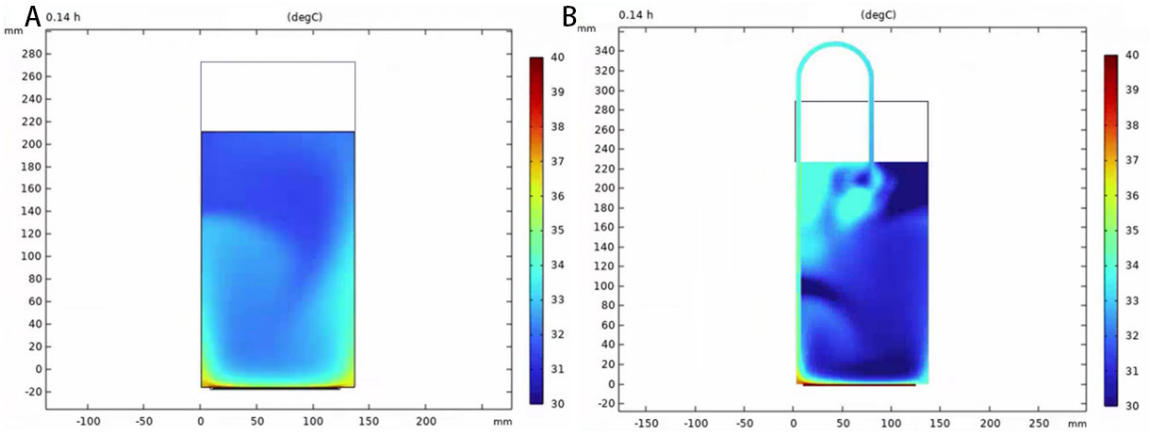

Figure 4. Heat distribution in the water infusion container model at 0.14 h. (A) Natural heating mode; (B) Circulating heating mode.

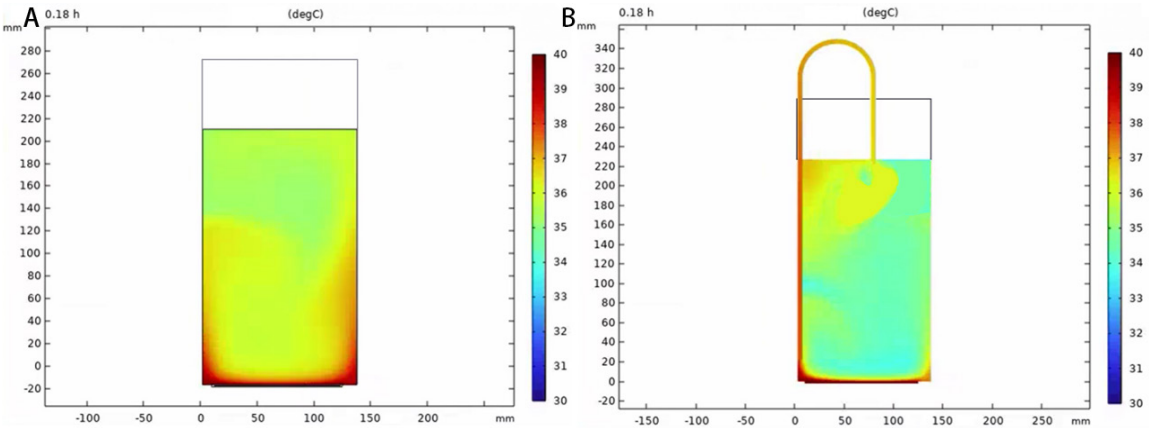

Figure 5. Heat distribution in the water infusion container model at 0.18 h. (A) Natural heating mode; (B) Circulating heating mode.

To prevent direct contact between the heater and the liquid during the diagnostic and therapeutic process, a silicone rubber heating sheet was employed in this study. The heating sheet is designed to be directly affixed to the bottom of the liquid container. It is made from a nickel-chromium alloy, a material with high resistivity, allowing it to self-generate heat when power is applied. This design offers flexibility, enabling customization to the shape and size of the container while ensuring uniform surface heating. Additionally, the heating sheet exhibits excellent thermal inertia, which enables gradual heat release, preventing local overheating and maintaining the stability and reliability of the heating process.

Temperature measuring circuit

In this study, negative temperature coefficient thermistors were primarily employed as temperature sensors to meet the measurement requirements. The sensor has a resistance value of 10K at room temperature, which varies with changes in the surrounding temperature, making it suitable for applications within the range of -55 °C to 300 °C [18]. The thermoplastic elastomer waterproof temperature probe is the actual sensor used, as it is compact enough to be integrated into a micro device and strategically positioned at a critical monitoring location within the container. The experimental setup includes a total of 12 pre-established temperature measurement points, with each sensor connected to the circuit control module via data transmission lines in the positioning bracket [19].

Temperature control circuit

The temperature control circuit developed in this study primarily consists of a PC817 optocoupler, an S8050 low-power NPN silicon transistor, and an SLA-12VC-SL-A relay. The circuit employs an electrical isolation drive scheme, as shown in **Figure 7**. It includes three main interfaces: the general purpose input/output control port on the left, which is directly connected to the main control circuit; the power

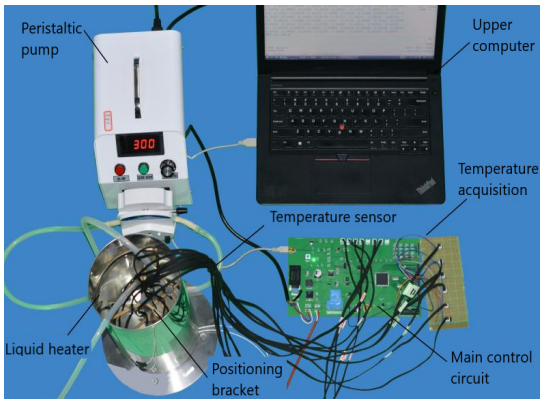

Figure 6. Prototype of the developed water infusion system.

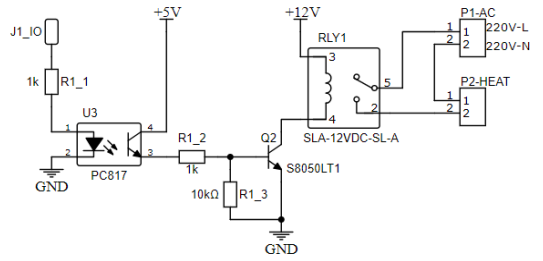

Figure 7. Temperature control circuit of the developed water infusion system. GND, Ground.

input port for 220 V AC; and the connection port for the heating component [20].

Upper computer display

This study employs LabVIEW software to develop an upper computer program for display purposes. The program facilitates real-time monitoring and management of the lower electrical circuit and its operational status. The system interface and component block diagram are shown in **Figure 8** and **Figure 9**, respectively. The software platform includes indicators, drawing tools, and user components. Various communication protocols supported by LabVIEW are utilized to configure parameters, collect temperature data, plot real-time change curves, and perform other core functions [21].

PID algorithm

To achieve precise temperature control, this study primarily employs the PID algorithm within the control system. The PID equation (using the coefficient method) is applied for this purpose.

$$u(k) = Kp * (e(k) - e(k-1)) + Ki * e(k) + Kd * (e(k) - 2e(k-1) + e(k-2))$$

In the equation, u (k) represents the controller output, while e (k) denotes the control deviation. The numerical signal is transmitted to the main control chip through the general purpose input/output port via the temperature acquisition circuit, and the PID calculation is performed in milliseconds [22]. Subsequently, the pulse width modulation (PWM) generator is used to adjust the heating power of the heating sheet. Once the proportional coefficient Kp, integral coefficient Ki, and derivative coefficient Kd are determined through calibration, the system is able to regulate the temperature of the static liquid with an error margin of less than 1 °C [23].

Functional verification and performance testing

Experimental setup

To implement the system, the following steps should be taken: First, activate the power module switch to initiate the system and bring the device to a ready state. Second, activate the pressure sensors to monitor the water injection process. The control panel will immediately display the amount of water injected into the liquid container, while the system will maintain minimum and maximum alarm limits for the water level. If the liquid level drops below the minimum threshold, a continuous beep will sound until the level rises above this threshold.

The system also includes a maximum water level alarm to prevent overflow, with the maximum water level set at 4 L for the container in use. Once the liquid reservoir is filled, the heating temperature can be preset using the control panel button, and the pump speed can be adjusted. After completing the preparation, open the second valve to initiate the internal circulation function. Once the device is started, the heating system should be activated to begin the heating process. This will cause the bottom heating element to rapidly heat the liquid to the desired temperature. Temperature distribution within the liquid can be closely monitored using the temperature measurement points, numbered from No. 1 to No. 12, located on the positioning bracket, as shown in **Figure 10**.

During the experiment, the core components of the temperature control system operated continuously to monitor the liquid temperature and transmit data to the central control unit in real time. The system automatically adjusts the operation of the heating device using an advanced control algorithm, which compares the real-time temperature with the preset target value. To ensure the precision of the

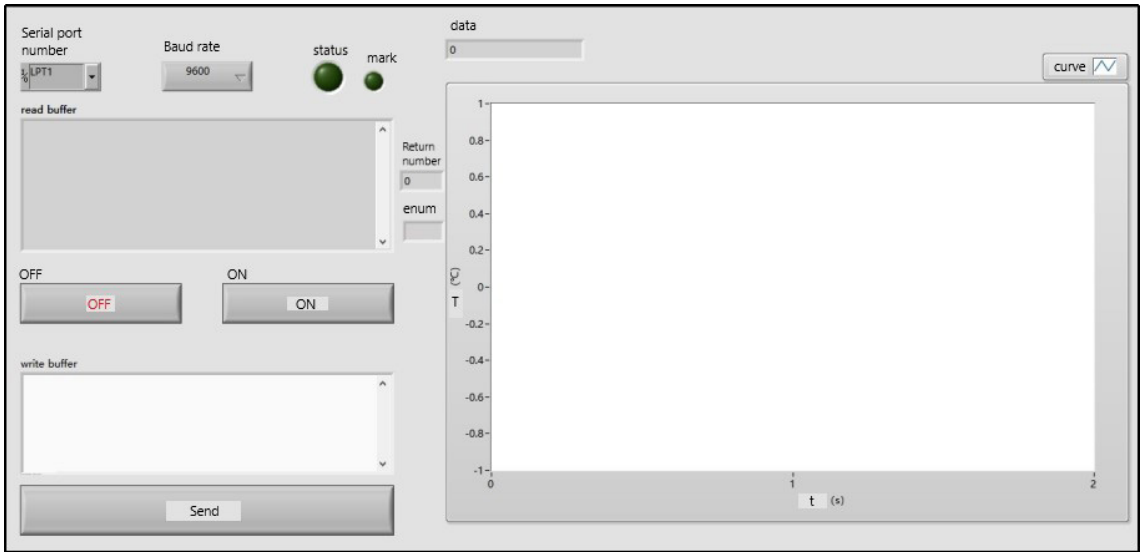

Figure 8. System interface of the developed water infusion system.

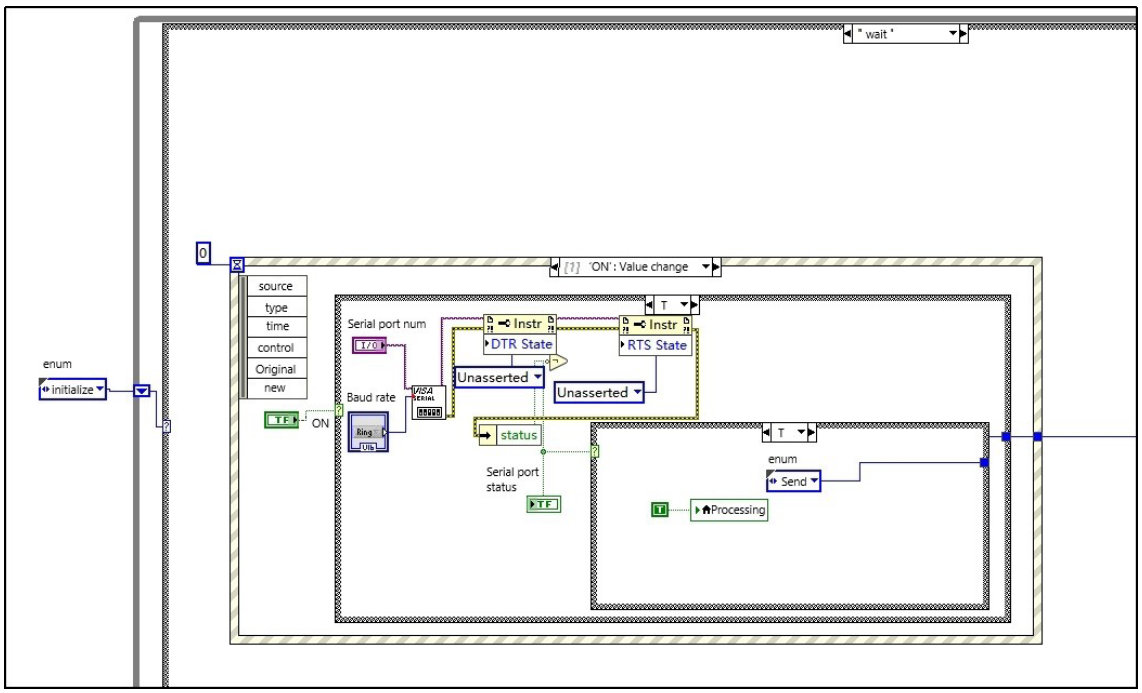

Figure 9. Component block diagram of the developed water infusion system.

experiment, the No. 1 valve remains closed until the liquid temperature reaches the required conditions. Once the liquid temperature reaches the target value, a progress indicator appears on the control panel, signaling the operator to manually initiate the water injection process. This involves adjusting the No. 1 valve and the pump speed control to accurately inject water into the simulated intestine through the injection port.

Results

Finite element simulation results

After conducting a comprehensive evaluation of the thermostatic heating system's performance, significant conclusions were drawn, particularly regarding the heating mode with constant temperature control. When relying solely on control for heating, the slow natural convection within the liquid leads to inefficient heat transfer, resulting in uneven temperature distribution. The maximum temperature difference can reach up to 5 °C, highlighting the limitations of a single thermostatic control mode in maintaining a uniform internal liquid temperature.

To address this issue, a proposal was made to

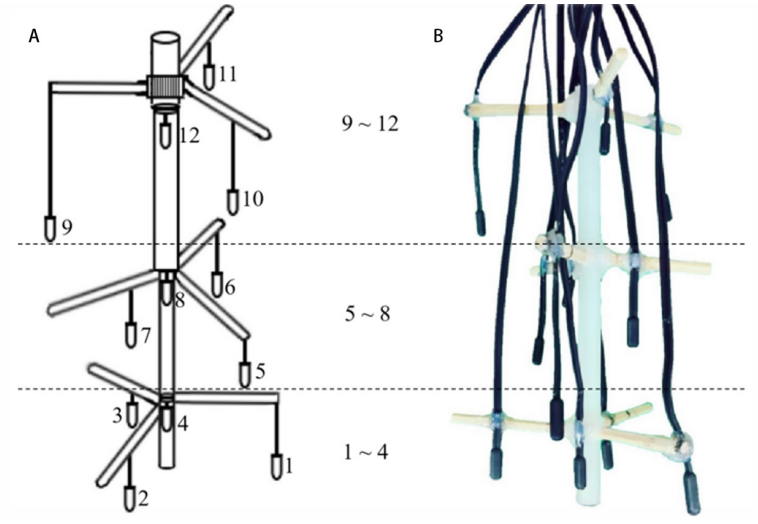

Figure 10. Multi-point temperature measurement stent for prototype performance testing. (A) Layout drawing; (B) Physical connection.

enhance heat transfer by increasing the return flow of the pipeline as an auxiliary measure. This approach accelerates temperature equalization by enhancing liquid heat circulation during heating, reducing the maximum temperature difference to approximately 1 °C. This not only visually illustrates the temperature variation between the upper and lower levels in the natural heating mode but also highlights the importance of pipeline reflux in improving the accuracy of liquid temperature control. Furthermore, the circulating method results in significantly more consistent liquid heat distribution compared to a simulation model without the circulating pipe and valve system.

Experimental platform results

In this study, the initial temperature of the liquid was set to approximately 25.5 °C, reflecting the ambient room temperature. The liquid volume was maintained at a constant 3.5 L, with a target temperature of 37 °C, designed to simulate the internal temperature of an organism. To ensure data accuracy and system stability, any extreme outliers were excluded from the temperature measurements. The temperature difference ($\Delta t = t_{max} - t_{min}$) was then calculated based on the highest and lowest values from the remaining data.

The experiment identifies two key time points: t1, which marks the onset of significant temperature fluctuations (ΔT exceeding approximately 0.5 °C), indicating the responsiveness of the heating system; and t2, which represents the time required for the system to reach the target temperature (T_{set}), determined by the mean of the remaining 10 temperature readings. This time point serves as an indicator of the system's efficiency in raising the water temperature to the desired level. This analysis aims to provide a comprehensive understanding of the dynamic response of the temperature control system and its ability to adapt to varying experimental conditions, thereby informing enhancements in the design and operational strategies of the experimental setup.

The study focuses on monitoring the maximum and minimum temperatures during the heating process, as well as the variations in the maximum temperature difference between them. Dynamic temperature changes at 200 W without pump-assisted convection are shown in **Figure 11**. This figure highlights the natural temperature distribution pattern in the absence of external forces and emphasizes the potential maximum temperature gradient under these conditions. The optimal configuration, identified after screening, involves circulating heating at 200 W power and 300 rpm, as shown in **Figure 12**. The temperature fluctuations observed in this setup demonstrate how precise control of heater power and pump speed can enhance the uniformity and efficiency of the heating process.

The system's thermal dynamic response characteristics were analyzed during initial startup under specific experimental environmental conditions, including normal atmospheric pressure and room temperature (25 °C). Analysis of the experimental data revealed an initial lack of significant temperature change in both liquid groups, which can be attributed to inherent system response time delays and heat transfer buffering effects. This indicated limited heat conduction efficiency at the onset of system operation, leading to a transient temperature stability phase. However, after approximately 50 seconds, a noticeable temperature increase was observed in both experimental conditions. Subsequently, the liquid temperature exhibited a trend toward stabilization, eventually reaching a relatively constant state. The temperature fluctuations around the designated value indicated that the system had achieved thermal equilibrium.

The pump body was not employed for heating in the experimental group. As a result, the gradual

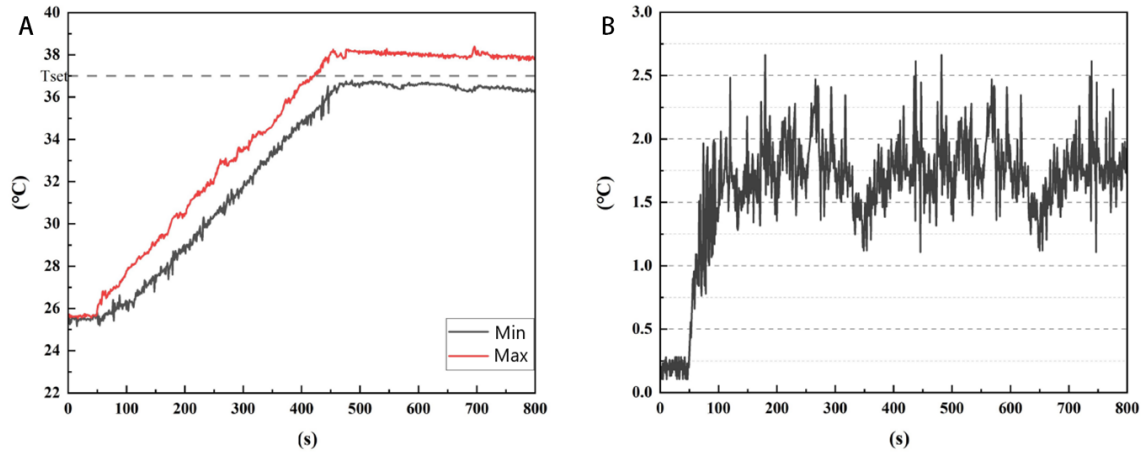

Figure 11. Temperature variation of the prototype water infusion device at 200 W, 0 rpm. (A) Minimum maximum temperature; (B) Maximum temperature difference.

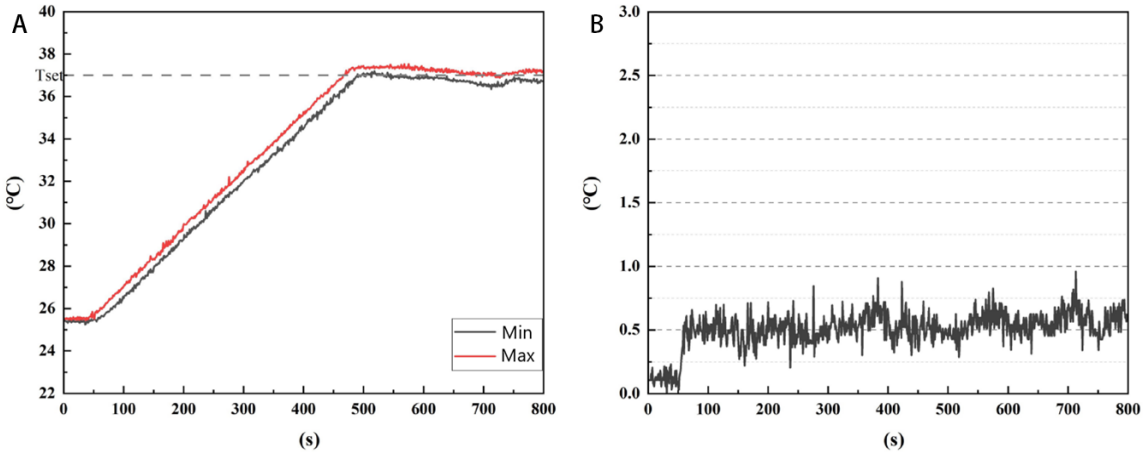

Figure 12. Temperature variation of the prototype water infusion device at 200 w, 300 rpm. (A) Minimum maximum temperature; (B) Maximum temperature difference.

increase in liquid temperature led to increasing inhomogeneity in temperature distribution. This was evident from the significant rise in the temperature difference between the highest and lowest recorded points, which reached a maximum of approximately 1.8 °C, with isolated instances exceeding 2.6 °C. The fluctuation underscores how the absence of the pump body significantly affects liquid temperature distribution. Around 8 minutes into the experiment, a notable inflection point was observed in the temperature data from the two measurement points, indicating that the liquid temperature was approaching the target temperature (T_set), eventually achieving the preset value of 37 °C. Although the liquid temperature stabilized thereafter, a noticeable disparity between the highest and lowest temperatures remained.

Analysis of the two temperature measurement points revealed a significant reduction in internal temperature variation after heating, at approximately 0.4 °C, underscoring the circulating heating system's effectiveness in enhancing heating uniformity. Once the target temperature (T_set) was reached, the temperature difference stabilized at approximately 0.5 °C, despite a brief overshoot in the maximum reading. As the experiment progressed, the temperature difference between the two measurement points gradually diminished, ultimately converging to near uniformity.

Discussion

This study focused on the development of a 37 °C water infusion device for colonoscopy diagnosis and treatment, addressing several key research and development issues. Firstly, it was demonstrated that the circulating heating mode, as opposed to natural convection heating, enhances heating efficiency and ensures uniform temperature distribution of the infusion water. Secondly, the device effectively

maintains a steady 37 °C temperature for the infusion water in room temperature settings.

In the finite element simulation section of this study, two distinct heating modes were compared for liquid containers: natural convection heating mode and cyclic uniform temperature control heating mode. The comparison aimed to assess heating efficiency and temperature distribution uniformity between the two modes.

The numerical simulation results indicated that the circulating uniform-temperature control heating mode exhibited significant advantages. A temperature control scheme combining a PID control algorithm with PWM technology was utilized in the prototype development. This scheme integrates the precise adjustment capabilities of the PID algorithm with the dynamic power output control enabled by PWM technology. It not only allows for efficient regulation of system heating power but also optimizes energy utilization and reduces system energy consumption. Compared to traditional PID technology, this combined approach offers more precise control by linking the PID output with the PWM duty cycle. This integration allows the system to respond more quickly to changes, thereby enhancing the dynamic performance of the system.

By appropriately adjusting the pump flow rate and implementing this temperature control scheme, the continuity and uniformity of the infusion water heating process can be maintained, ensuring safety, quality, and improved patient tolerance during endoscopic diagnostic and treatment procedures.

Conclusion

In this study, a device was developed to provide constant-temperature water for WAC via water infusion. The device underwent functional verification and performance evaluation through both numerical simulation and prototype testing. Simulation results demonstrated that the cyclic uniform heating mode, as opposed to natural convection heating, significantly enhances heating efficiency and ensures more uniform infusion water temperature. Prototype testing further confirmed that the temperature control scheme-integrating PID control with PWM technology-offers superior accuracy, rapid response, and stability. The implementation of 37 °C constant-temperature water infusion in WAC is expected to significantly improve the efficiency, safety, and patient satisfaction associated with endoscopic procedures.

However, several aspects of this study remain to be fully explored. To address these limitations, future work will focus on the following areas for improvement and further discussion. Subsequent research may consider incorporating fuzzy control technology to optimize the control process and enhance the system's resistance to external disturbances. Additionally, the adoption of multiple control schemes is proposed, allowing operators to control functions-such as starting and stopping the water infusion system-without the need for manual operation.

Author contributions: Hongsheng Li: Writing-original draft, Methodology, Investigation, Formal analysis, Data curation. Chunhua Zhou: Conceptualization, Writing-review and editing. Taojing Ran: Writing-review and editing. Yao Zhang: Investigation, Data curation. Xiaonan Shen: Investigation, Data curation. Shiju Yan: Conceptualization, Supervision, Writing-review and editing. Duowu Zou: Conceptualization, Supervision, Funding acquisition.

References

[1] Bray F, Ferlay J, Soerjomataram I, et al. Global cancer statistics 2018: GLOBOCAN estimates of incidence and mortality worldwide for 36 cancers in 185 countries. CA Cancer J Clin 2018;68(6):394-424.

[2] Davidson KW, Barry MJ, Mangione CM, et al. Screening for Colorectal Cancer: US Preventive Services Task Force Recommendation Statement. Jama 2021;325(19):1965-1977.

[3] Issaka RB, Chan AT, Gupta S. AGA Clinical Practice Update on Risk Stratification for Colorectal Cancer Screening and Post-Polypectomy Surveillance: Expert Review. Gastroenterology 2023;165(5):1280-1291.

[4] Leung CW, Kaltenbach T, Soetikno R, et al. Water immersion versus standard colonoscopy insertion technique: randomized trial shows promise for minimal sedation. Endoscopy 2010;42(7):557-563.

[5] Hsieh YH, Tseng CW, Hu CT, et al. Prospective multicenter randomized controlled trial comparing adenoma detection rate in colonoscopy using water exchange, water immersion, and air insufflation. Gastrointest Endosc 2017;86(1):192-201.

[6] Cadoni S, Ishaq S. How to perform water-aided colonoscopy, with differences between water immersion and water exchange: a teaching video demonstration. VideoGIE 2018;3(5):169-170.

[7] Leung FW. Methods of reducing discomfort during colonoscopy. Dig Dis Sci

2008;53(6):1462-1467.
[8] Terruzzi V, Paggi S, Amato A, et al. Unsedated colonoscopy: A neverending story. World J Gastrointest Endosc 2012;4(4):137-141.
[9] Chen Z, Li Z, Yu X, et al. Is water exchange superior to water immersion for colonoscopy? A systematic review and meta-analysis. Saudi J Gastroenterol 2018;24(5):259-267.
[10] Hsieh Y, Tseng C, Koo M, et al. Feasibility of sedation on demand in Taiwan using water exchange and air insufflation: A randomized controlled trial. J Gastroenterol Hepatol 2020;35(2):256-262.
[11] Hsieh YH, Koo M, Leung FW. A patient-blinded randomized, controlled trial comparing air insufflation, water immersion, and water exchange during minimally sedated colonoscopy. Am J Gastroenterol 2014;109(9):1390-1400.
[12] Khan R, Ruan Y, Yuan Y, et al. Relative Efficacies of Interventions to Improve the Quality of Screening-Related Colonoscopy: A Systematic Review and Network Meta-Analysis of Randomized Controlled Trials. Gastroenterology 2024;167(3):560-590.
[13] El Rahyel A, McWhinney CD, Parsa N, et al. Room temperature water infusion during colonoscopy insertion induces rectosigmoid colon mucus production. Endoscopy 2020;52(12):1118-1121.
[14] Falt P, Šmajstrla V, Fojtík P, et al. Cool water vs warm water immersion for minimal sedation colonoscopy: a double-blind randomized trial. Colorectal Dis 2013;15(10):e612-617.
[15] Calcara C, Aseni P, Siau K, et al. Water immersion sigmoidoscopy versus standard insufflation for colorectal cancer screening: A cohort study. Saudi J Gastroenterol 2022;28(1):39-45.
[16] Leung FW, Leung JW, Mann SK, et al. The water method significantly enhances patient-centered outcomes in sedated and unsedated colonoscopy. Endoscopy 2011;43(9):816-821.
[17] Oyetoke OO. A practical application of ARM Cortex-M3 processor core in embedded system engineering. Int J Intell Syst Appl 2017;9(7):70-88.
[18] Liu G, Guo L, Liu C, et al. Evaluation of different calibration equations for NTC thermistor applied to high-precision temperature measurement. Measurement 2018;120:21-27.
[19] Kharitonov OV, Firsova LA. Separation Features of TPE and REE by Complex Displacement Chromatography from Highly Active Solutions Formed after SNF Processing. Radiochemistry 2022;64(6):721-727.
[20] Zong X, Zhang J-F, Zheng J, et al. Design of boundary pulse width modulation controller for a class of heat equations. Appl Math Comput 2023;437:127511.
[21] Hao H, Zhang HL. Design of flow measurement system based on LabVIEW. IOP Conference Series: Materials Science and Engineering 2020;789:012027.
[22] Meng J, Gao H, Ruan M, et al. Design of vacuum annealing furnace temperature control system based on GA-Fuzzy-PID algorithm. Plos One 2023;18(11):e0293823.
[23] Singgih H, Siswoko S, Komarudin A. Study of PID control implementation in the process of cheap breaking using Peltier cooling elements. IOP Conference Series: Materials Science and Engineering 2020;732:012061.